ASME Paper Title: Dynamic Strength of Molecular Bond Clusters Under Displacement- and Force-Controlled Loading Conditions

Authors: Li, L., Yao, H., & Wang, J.

ASME Journal Title: The Journal of Applied Mechanics

Volume/Issue 83(2) Date of Publication (VOR* Online) November 11, 2015

ASME Digital Collection URL: https://asmedigitalcollection.asme.org/appliedmechanics/article/83/2/021004/442298/Dynamic-Strength-of-Molecular-Bond-Clusters-Under

DOI: https://doi.org/10.1115/1.4031802

The following publication Li, L., Yao, H., & Wang, J. (2016). Dynamic strength of molecular bond clusters under displacement-and force-controlled loading conditions. Journal of Applied Mechanics, 83(2), 021004 is available at https://doi.org/10.1115/1.4031802.

Dynamic strength of molecular bond clusters under displacement- and force-controlled loading conditions

Long Li
Key Laboratory of Mechanics on Disaster and Environment in Western China, Ministry of Education, College of Civil Engineering and Mechanics, Lanzhou University, Lanzhou, Gansu 730000, China
Department of Mechanical Engineering, the Hong Kong Polytechnic University, Hung Hom, Kowloon, Hong Kong SAR, China

Haimin Yao
Department of Mechanical Engineering, the Hong Kong Polytechnic University, Hung Hom, Kowloon, Hong Kong SAR, China

Jizeng Wang[1]
Key Laboratory of Mechanics on Disaster and Environment in Western China, Ministry of Education, College of Civil Engineering and Mechanics, Lanzhou University, Lanzhou, Gansu 730000, China
e-mail: jzwang@lzu.edu.cn

ABSTRACT

Existing experimental and theoretical studies on the adhesion of molecular bond clusters are usually based on either displacement- or force-controlled loading conditions. Very few studies have addressed whether or not and how the loading conditions affect the stochastic behavior of clusters. By considering the reversible breaking and rebinding process of ligand-receptor bonds, we directly solve the master equation about reactions between receptor-ligand bonds and conduct the corresponding Monte Carlo simulation to investigate the rupture forces of adhesion molecular clusters under linearly incremented displacement and force loading, respectively. We find that the rupture force of clusters strongly depends on loading conditions. Bond breaking and rebinding are independent of each other under displacement-controlled loading, whereas the rupture force highly depends on the state of each single bond under force-controlled

---

[1] Corresponding author.

loading. The physical mechanism of the dependence of rupture force on loading rate is also analyzed. We identify three reaction regimes in terms of loading rate: the regimes of equilibrium breaking/rebinding reactions, near equilibrium reaction, and far from equilibrium with only bond breaking. These findings can help improve the current understanding of the stochastic behaviors of the adhesion clusters of molecular bonds under dynamic loading conditions.

INTRODUCTION

As a fundamental biological process, cell adhesion has a pivotal role in their physiological and pathological functions, such as migration, growth, differentiation, and other multi-cellular events [1–3]. The receptors on the surface of cell membranes form many complexes with specific ligand molecules to enable the cell to sense its extracellular mechanical environment. These multiple receptor-ligand bonds are called adhesion clusters. The interactions between receptor and ligand molecules are typically weak. They form non-covalent bonds which can lead to reversible reactions. Receptor–ligand binding generally functions as a mechanical linker between the cytoskeleton and extracellular environments and is influenced by the mechanical loadings of blood flow, cytoskeleton contraction, and other factors. Through these linkers, cells can actively and passively sense and response to the environment. Therefore, the influence of mechanical loads on the biomechanical behaviors of receptor–ligand interactions must be examined to enhance our fundamental biological knowledge.

Numerous experimental measurements by means of atomic force microscopy, optical tweezers, magnetic tweezers, and biomembrane force probes have been conducted over the past two decades to investigate the forced-driven dissociation process of single receptor–ligand bonds. The rupture force of single bond breaking follows a probability distribution that depends on the loading rate [4–6]. An average bond rupture force is usually introduced to evaluate the bond strength [7]. When a single receptor–ligand bond is stretched under a high loading rate, the average bond rupture force is scaled linearly with the logarithm of the loading rate [6]. However, under a low loading rate, the bond strength exhibits an asymptotical strength limit, which does not depend on the loading rate [8].

Many theoretical models have been developed to explain the mechanism of bond breaking under different loading rates. In the pioneering framework of Kramers' theory on receptor–ligand reaction, bond dissociation is regarded as a thermally activated barrier crossing [9]. In the case of external force acting on a single bond, Bell [10] extended Kramers' theory to develop a simple analytical formula for describing the bond dissociation kinetics and found that the applied force can linearly decrease the potential well depth. Based on Bell theory for the force dependence of single bond dissociation, Raible et al. [11] proposed a theoretical model to verify the linear relation between the average rupture force and the logarithm of loading rate under a high loading rate. Bell theory also shows that the average rupture force is close to 0 at ultralow loading rates [7]. By assuming sophisticated interactions between specific molecules, many more theoretical analyses [12-15] were conducted to understand the bond rupture behavior under dynamic loading, the mean rupture force from these models [12-15] still approaches to 0 at ultralow loading rates. However, this prediction contradicts the experimental observation, in which the average rupture force is finite [8].

To address such inconsistency, Li and Ji [16, 17] and Chen et al. [18] theoretically explored the strength of a single bond at ultralow loading rate by considering both the breaking and rebinding processes between the free receptor and ligand molecules. They [16–18] pointed out that rebinding and bond stiffness have important roles in the strength of bonds at ultralow loading rates. In addition, Friddle et al. [19] theoretically demonstrated that there exits different reaction regimes associated with different loading rates, which depends on the probe stiffness and interaction potential between specific molecules.

However, the above studies merely describe the dynamic strength of a single receptor–ligand bond. Given that cell adhesion always consists of a large number of receptor–ligand bonds, several studies have intensively examined the dynamic strength of adhesion clusters. By performing atomic force microscopy to measure the adhesive strength between ligand molecules covered on the cantilever tip and the receptors on the surface of fibroblast cells, Chen and Moy [20] found that such adhesive strength can be enhanced by the cooperative action of multiple receptor–ligand bonds. Sulcheck et al. [21] further demonstrated that the measured rupture forces obey the predictions of a Markovian model for multiple parallel biological bonds. Evans and Ritchie [7] theoretically investigated the dynamic strength of molecular adhesion bonds in a liquid environment. They determined bond strength to be a force that produces the most frequent failures in repeated tests of breakage and identified three dynamic regimes of loading rate. By considering various interaction potentials between specific molecules under different loading rates, similar dynamic regimes are found by Friddle et al. [22].

For the reversible binding/unbinding process of adhesion molecules, Seifert [23, 24] suggested a rate equation based on Kramers theory for predicting the dynamic strength of adhesive molecules. He found that rebinding events lead to a finite strength at a zero loading rate and posited the scaling laws for the rupture force versus the number of bonds as either linear (i.e., similar to a square root) or logarithmic. Li and Leckband [25] discussed in more detail the dependence of bond dynamic strength on receptor–ligand kinetics and showed that the competition among different time scales, such as the intrinsic relaxation time, loading rate, and kinetics of bonds, produces three loading regimes: equilibrium, near-equilibrium, and far-from-equilibrium regimes, respectively. Given that rebinding events rarely occur under a high loading rate, Erdamann et al. [26] experimentally and theoretically demonstrated the bimodal distribution of the rupture force by considering only the breaking process of the bonds. Zhang et al. [27] considered the coupling between different loading conditions and the anisotropic elastic property of the adhesion system.

In terms of loading methods, the aforementioned studies can be classified into displacement- [11, 16–18, 23–25, 27] and force-controlled [20, 26, 28] loading groups. Only a few studies have realized that different loading conditions may lead to different adhesion behaviors. As such, the issues of whether or not and how displacement- and force-controlled loading conditions influence the adhesion strength of molecular clusters remain unclear. By considering the reversible breaking and rebinding processes of ligand–receptor bonds, we theoretically and numerically investigate the rupture forces of adhesion molecular clusters under linearly incremented displacement and force loading, respectively.

Model

Fig. 1 shows the adhesion of two rigid bodies via a cluster of ligand–receptor bonds, with each bond idealized as a Hookean spring. The interfacial separation is denoted by δ. Parameters l_b and l_bind denote the rest length of free receptor molecules and reacting radius of ligand–receptor bonds, respectively. We consider either the displacement-controlled loading with velocity μ (m/s) or the force-controlled loading with velocity m (N/s).

The stochastic process of the adhesion clusters of molecular bonds under a specific loading can be assumed as a Markov process, as described by the following master equation [29]:

$$\frac{dp_n}{dt} = (n+1)k_\mathrm{off}\,p_{n+1} + \left(N_\mathrm{t} - (n-1)\right)k_\mathrm{on}\,p_{n-1} - \left(nk_\mathrm{off} + (N_\mathrm{t} - n)k_\mathrm{on}\right)p_n\,, \qquad (1)$$

where p_n is the probability of n bonds to be closed at time t, N_t is the total number of bonds between two opposing surfaces, and k_off denotes the individual bond dissociation rate, which increases exponentially with loading force f_s exerted on single bonds [10]:

$$k_\mathrm{off} = k_0 \exp\left(f_\mathrm{s}/f_\mathrm{b}\right), \qquad (2)$$

with f_b being a force scale of 4 pN [10], and k_0 being the spontaneous dissociation rate in the absence of a loading force. $1/k_0$ typically ranges from a second to approximately 100 s [30], depending on the well depth of the binding potential. The association rate k_{on} of the free receptor and ligand molecules can be given by [31–33]

$$k_{\mathrm{on}} = k_{\mathrm{on}}^{0} \frac{l_{\mathrm{bind}}}{Z} \exp\left(-\frac{k_{\mathrm{LR}} \Delta\delta^{2}}{2k_{\mathrm{B}}T} \right), \tag{3}$$

where k_{on}^{0} is the spontaneous association rate of open bonds with zero separation, k_{LR} the stiffness of bonds, k_{B} the Boltzmann constant, T the absolute temperature, and $\Delta\delta = \delta - l_{\mathrm{b}}$ the separation between free receptors and ligand molecules. The partition function Z can be expressed as [31–33]

$$Z(\Delta\delta) = \sqrt{\frac{\pi k_{\mathrm{B}}T}{2k_{\mathrm{LR}}}} \left(\mathrm{erf}\left(\Delta\delta \sqrt{\frac{k_{\mathrm{LR}}}{2k_{\mathrm{B}}T}} \right) + \mathrm{erf}\left(l_{\mathrm{b}} \sqrt{\frac{k_{\mathrm{LR}}}{2k_{\mathrm{B}}T}} \right) \right). \tag{4}$$

We consider all bonds are initially closed, i.e., $p_{n=N_{\mathrm{t}}}(0)=1$ and $p_{n \neq N_{\mathrm{t}}}(0)=0$. In addition, we assume boundary conditions, $p_{-1}(t)=0$ and $p_{N_{\mathrm{t}}+1}(t)=0$. Then the master equation (1) can be solved by using conventional numerical methods for initial value problems. Once the probability of n bonds closed at time t, $p_n(t)$, n=0, 1, 2, ..., N_{t}, respectively, is obtained, the average number of closed bonds can be determined by [29, 33]

$$N_{\mathrm{c}}(t) = \sum_{n=0}^{N_{\mathrm{t}}} n p_n(t). \tag{5}$$

In the following section, we will discuss the specific forms of reaction rates k_{off} and k_{on} under displacement- and force- controlled loading, respectively.

Displacement-controlled loading

Under a displacement-controlled loading condition and a constant incremental rate μ, the interfacial separation can be described as

$$\delta = l_{\mathrm{b}} + \mu t \, . \tag{6}$$

For closed bonds, each bond force can be expressed as

$$f_{\mathrm{i}} = k_{\mathrm{LR}} \Delta\delta = k_{\mathrm{LR}} (\delta - l_{\mathrm{b}}) = k_{\mathrm{LR}} \mu t \, , \tag{7}$$

where $\Delta\delta = \mu t$ represents the deformation of each closed bond. Therefore, substituting Eqs. (6) and (7) into Eqs. (2) to (3) yields the dissociation and association rates under linearly displacement-controlled loading as

$$\begin{cases} k_{\mathrm{off}}(t) = k_0 \exp(k_{\mathrm{LR}} \Delta\delta / f_{\mathrm{b}}) \\ k_{\mathrm{on}}(t) = k_{\mathrm{on}}^0 \dfrac{l_{\mathrm{bind}}}{Z(\Delta\delta)} \exp\left(- \dfrac{k_{\mathrm{LR}} \Delta\delta^2}{2 k_{\mathrm{B}} T} \right) \end{cases}, \text{ with } \Delta\delta = \mu t \, . \tag{8}$$

In displacement-controlled loading, the mean consultant interfacial force can be obtained by

$$F(t) = F_{\mathrm{d}}(t) = \Delta\delta k_{\mathrm{LR}} N_{\mathrm{c}}(t) = \mu t k_{\mathrm{LR}} \sum\nolimits_{n=0}^{N_{\mathrm{t}}} n p_n(t) \tag{9}$$

where $F(t)$ is shown in Fig. 1, and we use subscript "*d*" to represent the displacement-controlled loading condition.

The adhesion strength of the molecular clusters can be represented by the maximum value of this force during the loading history, $F_{\mathrm{d}}^{\max}$, which is also named rupture force.

Force-controlled loading

In the force-controlled loading condition, the stochastic behavior of molecular bonds becomes dependent on each other given that the applied force is always equally shared by all closed bonds. The force acting on each individual bond is given by

$$f_{\mathrm{i}} = \frac{F_{\mathrm{f}}(t)}{n(t)} = \frac{F(t)}{n(t)} = \frac{mt}{n(t)} \tag{10}$$

where $F_{\mathrm{f}} = F = mt$ is the applied external force. The bond deformation can be written as

$$\Delta\delta(t) = \delta(t) - l_{\mathrm{b}} = \frac{f_{\mathrm{i}}(t)}{k_{\mathrm{LR}}} = \frac{mt}{k_{\mathrm{LR}} n(t)}\,. \tag{11}$$

From Eq. (11) we can see that $\Delta\delta(t)$ is always a function of time, no matter whether the loading force is a constant or not.

Substituting Eqs. (10) and (11) into the bond dissociation and association rates in Eqs. (2) and (3) yields

$$\begin{cases} k_{\mathrm{off}}(t) = k_0 \exp\left(k_{\mathrm{LR}} \Delta\delta / f_{\mathrm{b}}\right) \\ k_{\mathrm{on}}(t) = k_{\mathrm{on}}^0 \dfrac{l_{\mathrm{bind}}}{Z(\Delta\delta)} \exp\left(-\dfrac{k_{\mathrm{LR}} \Delta\delta^2}{2k_{\mathrm{B}}T}\right) \end{cases}, \text{ with } \Delta\delta = \frac{mt}{k_{\mathrm{LR}} n}\,. \tag{12}$$

The average number of closed bonds, $N_{\mathrm{c}}(t)$, as a function of time can be obtained by numerically solving master Eqs. (1) and (5). After all the bonds are opened at time t^*, which is denoted as the cluster lifetime, the corresponding applied external force $F_{\mathrm{f}}(t^*) = mt^*$ is regarded as the dynamic strength under the force-controlled loading condition.

Monte Carlo simulation

In light of the first reaction method derived from the Gillespie algorithm [34, 35], the master equation Eq. (1) can also be numerically solved by using the Monte Carlo simulation. We adopt the following procedure to investigate the dependence of the adhesion strength of the molecular bond clusters on the loading conditions:

(1) All bonds are closed at time step 0 (i.e., $t = 0$).

(2) The exerted force for each closed bond and the separation for each open bond can be obtained by Eqs. (6, 7, 10, 11) in terms of force balance.

(3) For each individual binding site, a set of independent random numbers (ζ_{i}) that are uniformly distributed over [0, 1] are generated. The normalized reaction time for each binding site ($\tau_{\mathrm{i}} = t_{\mathrm{i}} k_0$) is calculated as [34, 35]

$$\tau_{\mathrm{i}} = -\ln \frac{\zeta_{\mathrm{i}}}{a_{\mathrm{i}}} \tag{13}$$

where a_{i} is the normalized reaction rate that depends on the bond states (i.e., $a_{\mathrm{i}} = k_{\mathrm{off}} / k_0$ for closed bond and $a_{\mathrm{i}} = k_{\mathrm{on}} / k_0$ for open bond). k_{off} and k_{on} are computed by Eqs. (8) and (12), which are corresponding to the displacement- and force- controlled loading conditions, respectively. The smallest time $d\tau = \min(\tau_{\mathrm{i}})$ is recorded as the actual reaction time, which is associated with the next bond reaction. The bond state with the shortest reaction time is changed, and the adhesion lifetime is recorded as $\tau = \tau + d\tau$.

(4) Step 2 is repeated until all the bonds are in the open state.

We adopt the following parameters: bond stiffness k_{LR} = 0.5 pN/nm [36], bond rest length l_{b} = 11 nm [33], reacting radius of the binding site l_{bind} = 1 nm [33], total number of binding sites N_t = 100, absolute temperature T = 310 K, dissociation rate of unstressed bond k_0 = 2 s^{-1} [30], and intrinsic association rate of bond $k_{\mathrm{on}}^{0} = 1000$ s^{-1} [37].

Results and discussions

Fig. 2 plots the predicted normalized closed bonds number (N_c/N_t) as a function of time for different loading rates under displacement- (Fig. 2a) and force-controlled (Fig. 2b) loading conditions. The lifetime of the adhesion cluster strongly depends on the loading rate. Under a high loading rate, all initially closed bonds open for a short period. Fig. 3 shows the interfacial force as a function of time under displacement- (Fig. 3a) and force-controlled (Fig. 3b) loading conditions at different loading rates. Fig. 3 shows some of the differences between the curves of adhesion force and time for the molecular bond clusters under displacement- and force-controlled loadings. The adhesion force under force-controlled loading is sharply decreased after reaching the maximum value. The theoretical results are in excellent agreement with the corresponding Monte Carlo simulations in Figs. 2 and 3.

Given that rupture force is the maximum adhesion force, Fig. 4 shows the rupture force as a function of loading rate under displacement- and force-controlled loading conditions. The rupture force of the adhesion cluster of molecular bonds has a weak dependence on the loading methods at a low loading rate. However, the loading methods have significant effects on the rupture force at a high loading rate.

Eqs. (6) to (8) show that the rupture behavior of a bond is independent of that of another bond under the displacement-controlled loading condition. Therefore, the strength of the adhesion cluster of molecular bonds is denoted as the total strength of all the bonds. However, the bond rupture behavior under the force-controlled loading condition is no longer independent. Instead, the breaking and rebinding events of each bond becomes strongly dependent on the binding and deformation states of all the other bonds. Such difference has been observed by Zhang et al. [27] in examining the adhesion of anisotropic elastic media via molecular bond clusters.

Bond rebinding rarely takes place when the cluster of molecular bonds is subjected to a high loading rate. Therefore, the adhesion is dominated only by the breaking process of bonds. In this situation, the master Eq. (1) can be rewritten as

$$\frac{dp_n}{dt} = (n+1)k_{\mathrm{off}}\,p_{n+1} - nk_{\mathrm{off}}\,p_n \,. \tag{14}$$

Together Eqs. (5) and (14) gives the average number of closed bonds. The predicted relations between rupture force and loading rate under displacement- and force-controlled loading conditions are plotted in Fig. 4. These predictions, which are made by considering only the breaking process of the bonds and by considering both the breaking and rebinding processes of the bonds, show an excellent agreement with each other under a high loading rate. Therefore, considering only the breaking process of the bonds can describe the rupture behavior of the adhesion cluster under a high loading rate [26].

Bond breaking and rebinding occur constantly under an ultralow loading rate where all the receptor and ligand molecules have sufficient time to react and lead to a reaction equilibrium ($dp_n/dt = 0$). Hence, the master Eq. (1) can be rewritten as

$$(n+1)k_{\mathrm{off}}\,p_{n+1} + (N_{\mathrm{t}} - (n-1))k_{\mathrm{on}}\,p_{n-1} = (nk_{\mathrm{off}} + (N_t - n)k_{\mathrm{on}})p_n \,, \tag{15}$$

Distinguishing from high loading rate, under an ultralow loading rate the reaction rates are closed to constants at each time step as

$$\begin{cases} k_{\mathrm{off}}(t) = k_0 \exp\left(k_{\mathrm{LR}} \Delta\delta / f_{\mathrm{b}}\right) \\ k_{\mathrm{on}}(t) = k_{\mathrm{on}}^0 \dfrac{l_{\mathrm{bind}}}{Z} \exp\left(-\dfrac{k_{\mathrm{LR}} \Delta\delta^2}{2k_{\mathrm{B}}T}\right) \end{cases} \tag{16}$$

where term, $k_{\mathrm{LR}}\Delta\delta\sum_{n=0}^{N_{\mathrm{t}}} np_n(t)$, denotes the interfacial force. By numerically solving master Eqs. (15) and (16), Fig. 5 shows the applied force as a function of bond deformation at an ultralow loading rate. A constant critical rupture force, F_{c}, is also observed at an ultralow loading rate.

Figs. 4 and 5 identify three regimes of rupture force in terms of loading rate: equilibrium reaction regime, near equilibrium regime, and only bond breaking regime, which are shown in Fig. 6. Given that a sufficiently small loading rate is observed in the equilibrium reaction regime, a breaking/rebinding reaction may occur between the receptor–ligand molecules at any moment after they reach the equilibrium, thereby producing a constant rupture force as shown in Figs. 4 and 5. In the near equilibrium regime, the loading rates start to affect the rupture behavior of the adhesion cluster. In the only bond breaking regime, bond rebinding events are never observed, and the rupture force is scaled linearly with the logarithm of the loading rate.

Conclusion

By considering the reversible breaking and rebinding processes of adhesion bonds, we investigate the different rupture behaviors of adhesion clusters under displacement- and force-controlled loading conditions. Under displacement-controlled loading conditions, the rupture processes of the adhesion cluster are not observed during the stochastic coupling between two bonds, and the cluster rupture force is the summation of only that for each single bond. By contrast, under force-controlled loading conditions, the rupture process depends on the stochastic coupling between the behavior of each single bond, and the cluster rupture force is no longer the simple summation of that of each single bond. The statistical mechanism of the molecular bond cluster adhesion under dynamic loadings is also analyzed under high and low loading rates. Three regimes may affect how the loading rates influence the rupture force of the cluster. These results clearly show that the loading methods strongly influence the adhesion strength, shedding promising light on understanding of stochastic behaviors of the clusters of molecular bonds under dynamic loading conditions.

ACKNOWLEDGMENT

This study is supported by grants from the National Natural Science Foundation of China (11032006, 11121202). HY would like to acknowledge the support by the General Research Fund from Hong Kong RGC (Grant No. 15219314). LL would like to acknowledge the support by the Fundamental Research Funds for the Central Universities (lzujbky-2015-299).

REFERENCES

[1] Discher, D.E., Janmey, P., and Wang, Y.I., 2005, “Tissue cells feel and respond to the stiffness of their substrate,” Science, **310**(5751), pp. 1139-1143.

[2] Engler, .A.J., Sen, S., Sweeney, H.L., and Discher, D.E., 2006, “Matrix elasticity directs

stem cell lineage specification," Cell, **126**(4), pp. 667-689.

[3] He, S., Su, Y., Ji, B., and Gao, H., 2014, "Some basic questions on mechanosensing in cell–substrate interaction," J. Mech. Phys. Solids, **70**, pp. 116-135.

[4] Zhu, C., Long, M., Chesla, S.E., and Bongrand, P., 2002, "Measuring receptor/ligand interaction at the single-bond level: experimental and interpretative issues," Ann. Biomed. Eng., **30**(3), pp. 305-314.

[5] Lo, Y.S., Zhu, Y.J., and Beebe, T.P., 2001, "Loading-rate dependence of individual ligand-receptor bond-rupture forces studied by atomic force microscopy," Langmuir, **17**(2), pp. 3741-3748.

[6] Merkel, R., Nassoy, P., Leung, A., Ritchie, K., and Evans, E., 1999, "Energy landscapes of receptor–ligand bonds explored with dynamic force spectroscopy," Nature, **397**, pp. 50-53.

[7] Evans, E., and Ritchie, K., 1997, "Dynamic strength of molecular adhesion bonds," Biophys. J., **72**(4), pp. 1541-1555.

[8] Keten, S., and Buehler, M.J., 2008, "Asymptotic strength limit of hydrogen bond assemblies in proteins at vanishing pulling rates," Phys. Rev. Lett., **100**(19), p. 198301.

[9] Kramers, H.A., 1940, "Brownian motion in a field of force and the diffusion model of chemical reactions," Physica, **7**(4), pp. 284-304.

[10] Bell, G.I., 1978, "Models for the specific adhesion of cells to cells," Science, **200**(4342), pp. 618-627.

[11] Raible, M., Evstigneev, M., Reimann, P., Bartels, F.W., and Ros, R., 2004, "Theoretical analysis of dynamic force spectroscopy experiments on ligand–receptor complexes," J. Biotechnol., **112**(1-2), pp. 13-23.

[12] Bullerjahn, J.T., Sturm, S., and Kroy, K., 2014, "Theory of rapid force spectroscopy," Nat. Commun., **8**, p. 4463.

[13] Hummer, G., and Szabo, A., 2003, "Kinetics from nonequilibrium single-molecule pulling experiments," Biophys. J., **85**(1), pp. 5-15.

[14] Dudko, O.K., Hummer, G., and Szabo, A., 2006, "Intrinsic rates and activation free

energies from single-molecule pulling experiments," Phys. Rev. Lett., **96**, p. 108101.

[15] Maitra, A., and Arya, G., 2010, "Model accounting for the effects of pulling-device stiffness in the analyses of single-molecule force measurements," Phys. Rev. Lett., **105**, p. 259902.

[16] Li, D., and Ji, B., 2014, "Predicted rupture force of a single molecular bond becomes rate independent at ultralow loading rates," Phys. Rev. Lett., **112**(7), p. 078302.

[17] Li, D., and Ji, B., 2015, "Crucial Roles of Bond Rebinding in Rupture Behaviors of Single Molecular Bond at Ultralow Loading Rates," Int. J. Appl. Mech., **7**(1), p. 1550015.

[18] Chen, X., Li, D., Ji, B., and Chen, B., 2015, "Reconciling bond strength of a slip bond at low loading rates with rebinding," Europhysics Letters, **109**(6), p. 68002.

[19] Friddle, R.W., Podsiadlo, P., Artyukhin, A,B., and Noy, A., 2008, "Near-equilibrium chemical force microscopy," J. Phys. Chem. C, **112**, pp. 4986-4990.

[20] Chen, A., and Moy, V.T., 2000, "Cross-linking of cell surface receptors enhances cooperativity of molecular adhesion," Biophys. J., 78(6), pp. 2814-2820.

[21] Sulchek, T., Friddle, R.W., and Noy, A., 2006, "Strength of multiple parallel biological bonds," Biophys. J., **90**(12), pp. 4686-4691.

[22] Friddle, R.W., Noy, A., and Yoreo, J.J.D., 2012, "Interpreting the widespread nonlinear force spectra of intermolecular bonds," P. Natl. Acad. Sci. USA, **109**, PP. 13573-13578.

[23] Seifert, U., 2000, "Rupture of multiple parallel molecular bonds under dynamic loading," Phys. Rev. Lett., **84**(12), p. 2750.

[24] Seifert, U., 2002, "Dynamic strength of adhesion molecules: role of rebinding and self-consistent rates," Europhysics Letters, **58**(5), p. 792.

[25] Li, F., and Leckband, D., 2006, "Dynamic strength of molecularly bonded surfaces," J. Chem. Phys., **125**, p. 194702.

[26] Erdmann, T., Pierrat, S., Nassoy, P., and Schwarz, U.S., 2008, "Dynamic force spectroscopy on multiple bonds: Experiments and model," Europhysics Letters, **81**, p. 48001.

[27] Zhang, W.L., Lin, Y., Qian, J., Chen, W.Q., and Gao, H.J., 2013, "Tuning molecular adhesion via material anisotropy," Adv. Funct. Mater., **23**(37), pp. 4729-4738.

[28] Willemsen, O.H., Snel, M.M.E., Cambi, A., Greve, J., Grooth, B.G., and Figdor, C.G., 2000, "Biomolecular interactions measured by atomic force microscopy," Biophys. J., **79**(6), pp. 3267-3281.

[29] Erdmann, T., and Schwarz, U.S., 2004, "Stochastic dynamics of adhesion clusters under shared constant force and with rebinding," J. Chem. Phys., **121**(18), p. 8897.

[30] Evans, E.A., and Calderwood, D.A., 2007, "Forces and bond dynamics in cell adhesion," Science, **316**(5828), pp. 1148-1153.

[31] Erdmann, T., and Schwarz, U.S., 2007, "Impact of receptor-ligand distance on adhesion cluster stability," Eur. Phys. J. E, **22**(2), pp. 123-137.

[32] Erdmann, T., and Schwarz, U.S., 2006, "Bistability of cell-matrix adhesions resulting from nonlinear receptor-ligand dynamics," Biophys. J., **91**(6), pp. L60-L62.

[33] Qian, J, Wang, J.Z., and Gao, H.J., 2008, "Lifetime and strength of adhesive molecular bond clusters between elastic media," Langmuir, **24** (4), pp. 1262-1270.

[34] Gillespie, D.T., 1976, "A general method for numerically simulating the stochastic time evolution of coupled chemical reactions," J. Comput. Phys., **22**(4), pp. 403-434.

[35] Gillespie, D.T., 1977, "Exact stochastic simulation of coupled chemical reactions," J. Phys. Chem., **81**(25), pp. 2340-2361.

[36] Kong, F., Garcia, A.J., Mould, A.P., Humphries, M.J., and Zhu, C., 200, "Demonstration of catch bonds between an integrin and its ligand," J. Cell Biol., **185**(7), pp. 1275-1284.

[37] Bhatia, S.K., King, M.R., and Hammer, D.A., 2003, "The state diagram for cell adhesion mediated by two receptors," Biophys. J., **84**(4), pp. 2671-2690.

Figure legends

Figure 1. Schematic diagram of the separation of molecularly bonded surfaces under linear displacement loading with velocity μ or linear force loading with velocity m. l_b and l_{bind} are the rest length of the receptor and the reacting radius of the binding site, respectively. δ denotes the separation between two surfaces, and $\Delta\delta$ the distance between the free receptor and ligand molecule for the opened state and the deformation length of the bond for the closed state.

Figure 2. Normalized number of closed bonds N_c/N_t versus time for different loading rates with a total number of bonds $N_t = 100$: (a) linear displacement loading and (b) linear force loading. The theoretical results (solid lines) show excellent agreement with the Monte Carlo simulations (symbols).

Figure 3. Force acting on surfaces as a function of time for a total number of bonds $N_t = 100$ (lines: theoretical results; symbols: Monte Carlo simulations): (a) linear displacement loading and (b) linear force loading.

Figure 4. Rupture force of the adhesion cluster as a function of loading rate under linear displacement- and force-controlled loadings (lines: theoretical results; symbols: Monte Carlo simulations). μk_{LR} represents the loading rate under displacement loading. In the only bond breaking regime, the rupture forces are plotted as dash-dot lines for displacement loading and red dash lines for force loading. F_c is a critical rupture force. For any loading rate, the rupture force never decreases below the critical value.

Figure 5. At the equilibrium state of the receptor–ligand reactions, the surface force acts as a function of the stretched length of the receptor–ligand bond (lines: theoretical results; symbols: Monte Carlo simulations).

Figure 6. Different regimes of the rupture force of the adhesion cluster in terms of loading rate under linear force loading (lines: theoretical results; symbols: Monte Carlo simulations). The red line denotes the theoretical results based on the bond breaking model. The black line denotes the theoretical results from the current reversible breaking/rebinding model.

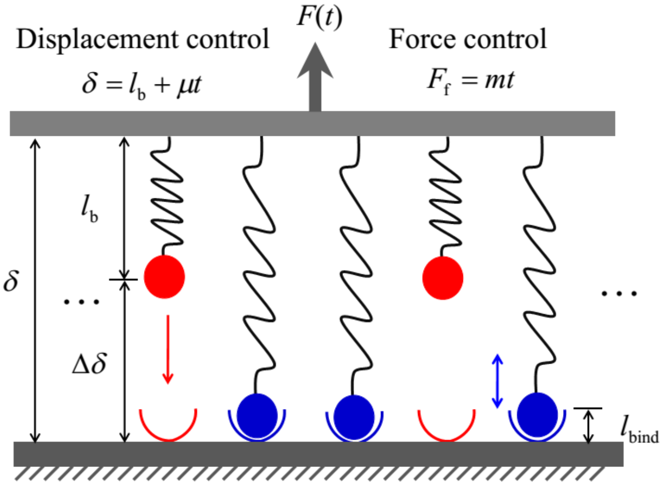
Displacement control
$\delta = l_b + \mu t$
$F(t)$
Force control
$F_f = mt$
l_b
δ
$\Delta\delta$
l_{bind}

Figure 1

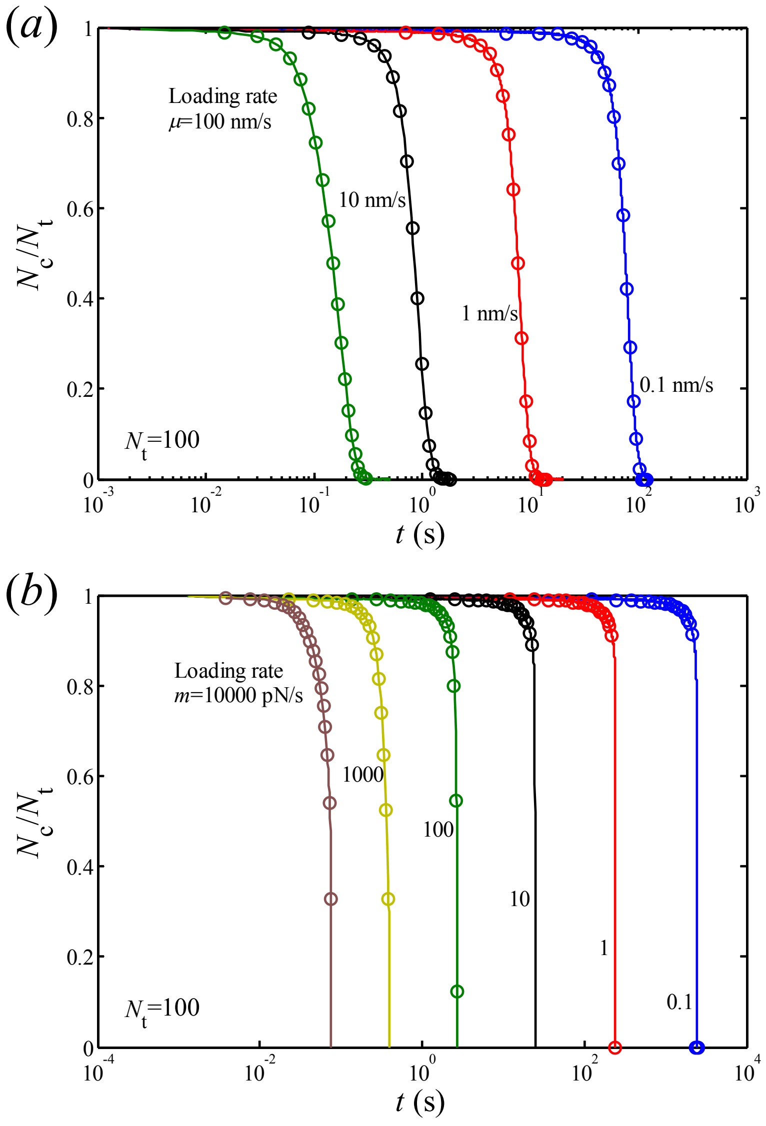
(a)
1
0.8
0.6
0.4
0.2
0
N_c/N_t
Loading rate
μ=100 nm/s
10 nm/s
1 nm/s
0.1 nm/s
N_t=100
10^{-3}
10^{-2}
10^{-1}
10^{0}
10^{1}
10^{2}
10^{3}
t (s)
(b)
1
0.8
0.6
0.4
0.2
0
N_c/N_t
Loading rate
m=10000 pN/s
1000
100
10
1
0.1
N_t=100
10^{-4}
10^{-2}
10^{0}
10^{2}
10^{4}
t (s)

Figure 2

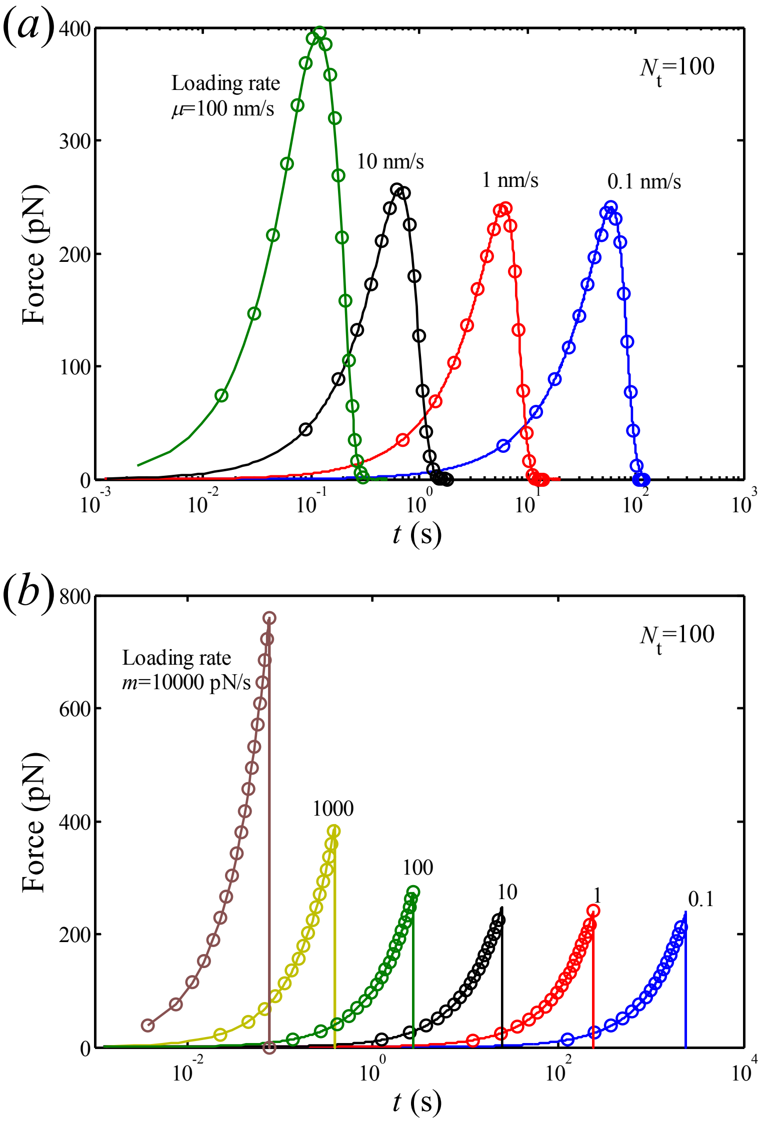
(a)
Force (pN)
t (s)
N_t=100
Loading rate
μ=100 nm/s
10 nm/s
1 nm/s
0.1 nm/s
0
100
200
300
400
10^{-3}
10^{-2}
10^{-1}
10^{0}
10^{1}
10^{2}
10^{3}
(b)
Force (pN)
t (s)
N_t=100
Loading rate
m=10000 pN/s
1000
100
10
1
0.1
0
200
400
600
800
10^{-2}
10^{0}
10^{2}
10^{4}

Figure 3

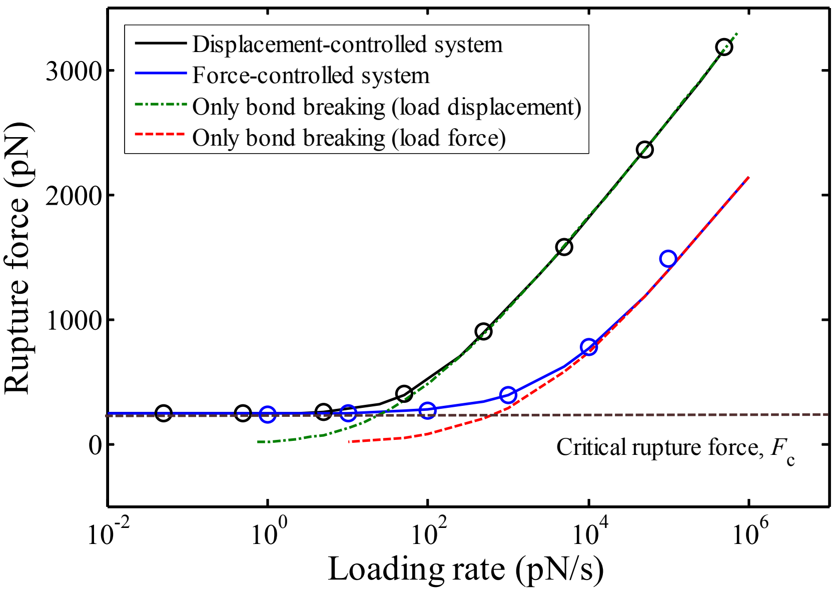
Displacement-controlled system
Force-controlled system
Only bond breaking (load displacement)
Only bond breaking (load force)
Rupture force (pN)
3000
2000
1000
0
Critical rupture force, F_c
10^{-2}
10^{0}
10^{2}
10^{4}
10^{6}
Loading rate (pN/s)

Figure 4

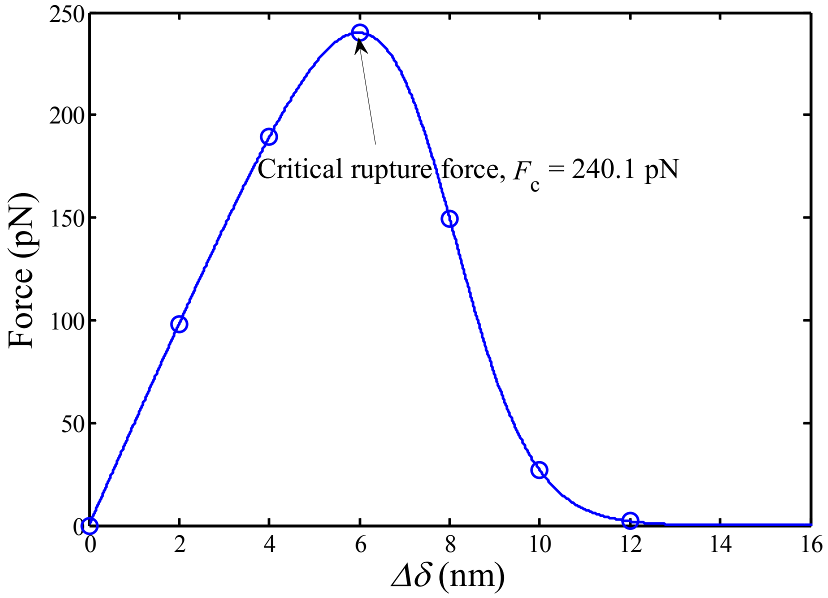
Force (pN)
0
50
100
150
200
250
Δδ (nm)
0
2
4
6
8
10
12
14
16
Critical rupture force, F_c = 240.1 pN

Figure 5

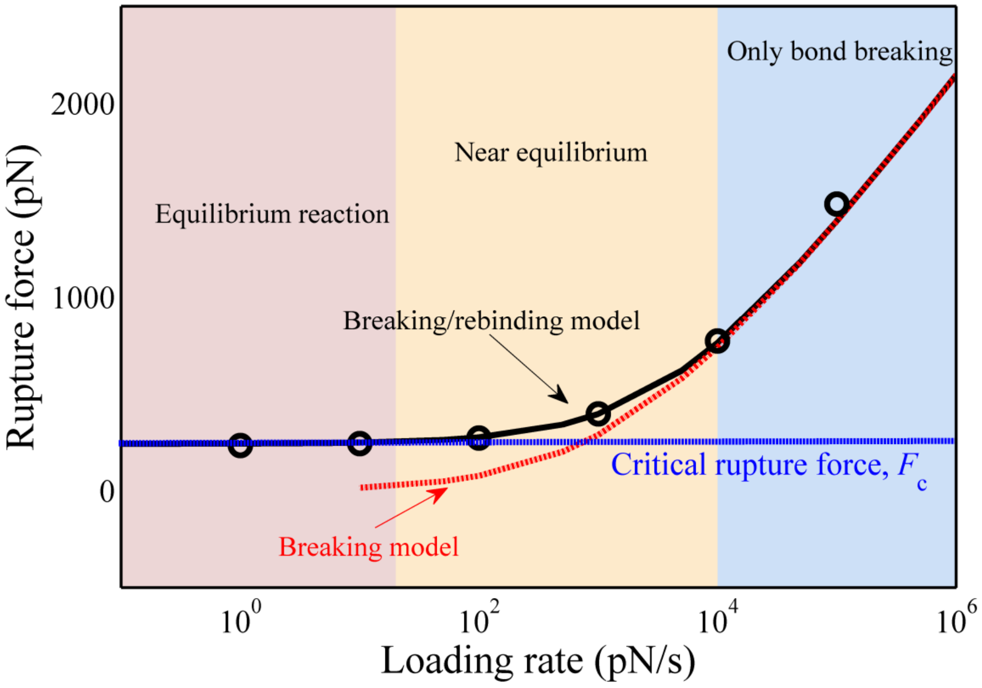
Only bond breaking
2000
Near equilibrium
Equilibrium reaction
1000
Breaking/rebinding model
Critical rupture force, F_c
0
Breaking model
Rupture force (pN)
10^0
10^2
10^4
10^6
Loading rate (pN/s)

Figure 6